Corrosion and Corrosion Inhibition of Mild Steel in Groundwater at Different Temperatures by Newly Synthesized Benzotriazole and Phosphono Derivatives

ARTICLE *in* INDUSTRIAL & ENGINEERING CHEMISTRY RESEARCH · MARCH 2014

Impact Factor: 2.59 · DOI: 10.1021/ie4039357

6 AUTHORS, INCLUDING:

El-Sayed M. Sherif
King Saud University
113 PUBLICATIONS **1,951** CITATIONS
SEE PROFILE

Manivannan Varadharajan
Thiruvalluvar Government Arts College, Rasip…
3 PUBLICATIONS **32** CITATIONS
SEE PROFILE

Kavitha Louis
Central University of Tamil Nadu
105 PUBLICATIONS **992** CITATIONS
SEE PROFILE

I&EC research
Industrial & Engineering Chemistry Research

Article

pubs.acs.org/IECR

Corrosion and Corrosion Inhibition of Mild Steel in Groundwater at Different Temperatures by Newly Synthesized Benzotriazole and Phosphono Derivatives

D. Gopi,*[,†,‡] El-Sayed M. Sherif,[§,∥] V. Manivannan,[⊥] D. Rajeswari,[†,#] M. Surendiran,[†] and L. Kavitha[¶]

[†]Department of Chemistry, Periyar University, Salem 636 011, Tamilnadu, India

[‡]Centre for Nanoscience and Nanotechnology, Periyar University, Salem 636 011, Tamilnadu, India

[§]Center of Excellence for Research in Engineering Materials (CEREM), Advanced manufacturing Institute, King Saud University, P.O. Box 800, Al-Riyadh 11421, Saudi Arabia

[∥]Electrochemistry and Corrosion Laboratory, Department of Physical Chemistry, National Research Centre (NRC), Dokki, 12622 Cairo, Egypt

[⊥]Department of Chemistry, Paavai College of Engineering, Namakkal 637 018, Tamilnadu, India

[#]Department of Physics, Periyar University, Salem 636 011, Tamilnadu, India

[¶]Department of Physics, School of Basic and Applied Sciences, Central University of Tamilnadu, Thiruvarur 610 101, Tamilnadu, India

Supporting Information

ABSTRACT: The corrosion and corrosion inhibition of mild steel in groundwater using 1-(2-pyrrolecarbonyl)-benzotriazole (PBTA) and 1-(2-thienylcarbonyl)-benzotriazole (TBTA) with 2-phosphonoacetic acid (PAA), 4-phosphonobutyric acid (PBA), and Zn^{2+} at various temperatures ranging from 30 to 60 °C were reported. The study was performed using potentiodynamic polarization (PDP) and electrochemical impedance spectroscopy (EIS) along with X-ray diffraction (XRD) and Scanning electron microscopy (SEM) investigations. PDP measurements proved that the presence of inhibitors decreases the corrosion of still by decreasing its corrosion current density. EIS data showed that the charge transfer resistance of steel increases in the groundwater containing inhibitors. XRD and SEM investigations confirmed that the inhibition of mild steel is achieved by the adsorption of the inhibitor molecules on the steel surface. All results indicated that the presence of PBTA and TBTA along with Zn^{2+} as well as PBA offered good inhibition efficiency against corrosion of mild steel in the groundwater media.

INTRODUCTION

In the past few decades, mild steel has been widely used in the fabrication of reaction vessels, storage tanks, petroleum refineries, etc. The corrosion of mild steel with its surrounding environment limits its uses in some of these applications. It has been reported[1] that one of the most effective methods of protecting mild steel against corrosion is the use of inhibitors, which are chemical substances that, when added in a small concentration, slow down the rate of corrosion. Therefore, the development and use of inhibitors to protect mild steel against corrosion in different corrosive media has attracted the attention of several investigators.[1−5] Organic compounds containing nitrogen, oxygen, sulfur, and heterocyclic rings are considered to be effective corrosion inhibitors; for instance, benzotriazole has been used as an inhibitor for the corrosion of mild steel, zinc, aluminum, and copper.[6−15] Among the various nitrogenous compounds, triazole derivatives have been considered as environmentally acceptable chemicals.[15]

Addition of small amounts of environmentally friendly organic additives to the phosphonic acid and metal cation blend was found to increase the corrosion inhibition of mild steel.[16] The phosphonates, when blended with certain metal cations and polymers, cause synergistic effects favorable for corrosion inhibition at low inhibitor concentrations.[17−19] In a previous work,[10] we investigated the effects of Zn^{2+}, 3-phosphonopropionic acid, benzotriazole, 1-(2-pyrrolecarbonyl)benzotriazole, and 1-(2-thienylcarbonyl)-benzotriazole on the inhibition of mild steel corrosion in groundwater using potentiodynamic polarization and electrochemical impedance spectroscopy along with X-ray diffraction and Fourier transform infrared spectroscopy. The study proved that there was a synergistic effect between the used benzotriazole and its derivatives with Zn^{2+}, which led to an effective combination in the inhibition of mild steel in the groundwater test solution.

In the present work, we extended our study to investigate the effects of 1-(2-pyrrolecarbonyl)benzotriazole (PBTA) and 1-(2-thienylcarbonyl)benzotriazole (TBTA) with 2-phosphonoacetic acid (PAA), 4-phosphonobutyric acid (PBA), and Zn^{2+} at various temperatures. The chemical structures of (a) PBTA, (b) TBTA, (c) PAA, and (d) BPA are shown in Figure 1. The objective was also to report the mechanism and quantitative correlation between the structures of the used inhibitors and

Received: November 19, 2013
Revised: February 24, 2014
Accepted: February 24, 2014
Published: February 24, 2014

dx.doi.org/10.1021/ie4039357 | Ind. Eng. Chem. Res. 2014, 53, 4286−4294

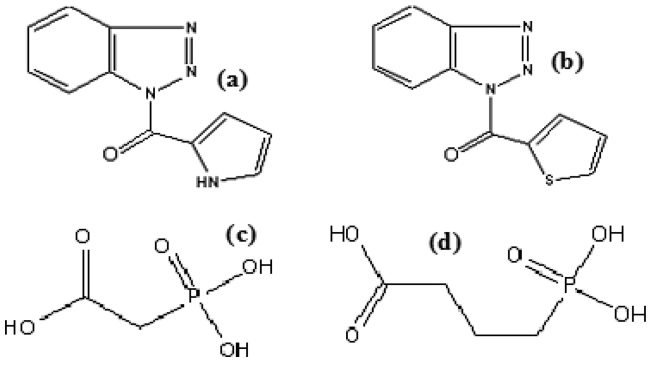

Figure 1. Chemical structures of (a) PBTA, (b) TBTA, (c) PAA, and (d) BPA, respectively.

their efficiencies at different temperatures. The study has been carried out using Fourier transform infrared, nuclear magnetic resonance, potentiodynamic polarization, and electrochemical impedance spectroscopy measurements and complemented by X-ray diffraction and scanning electron microscopy.

EXPERIMENTAL SECTION

Synthesis of Benzotriazole Derivatives. PBTA and TBTA were synthesized by adopting standard procedures as has been reported in previous studies.[11,20,21] In order to characterize the structure of the produced compounds, Fourier transform infrared (FT-IR) and nuclear magnetic resonance (NMR) investigations were carried out.

Electrochemical Cell and Chemicals. Groundwater was used as the electrolytic test solution and was collected at 10 different locations; it was then tested by the Langelier saturation index (LSI).[22] A typical chemical analysis of the used groundwater electrolytes is given in Table S1 (Supporting Information). A conventional electrochemical three-electrode configuration 200 mL cell was used with the mild steel as the working electrode, a platinum electrode as the counter (auxiliary) electrode, and a saturated calomel electrode (SCE)

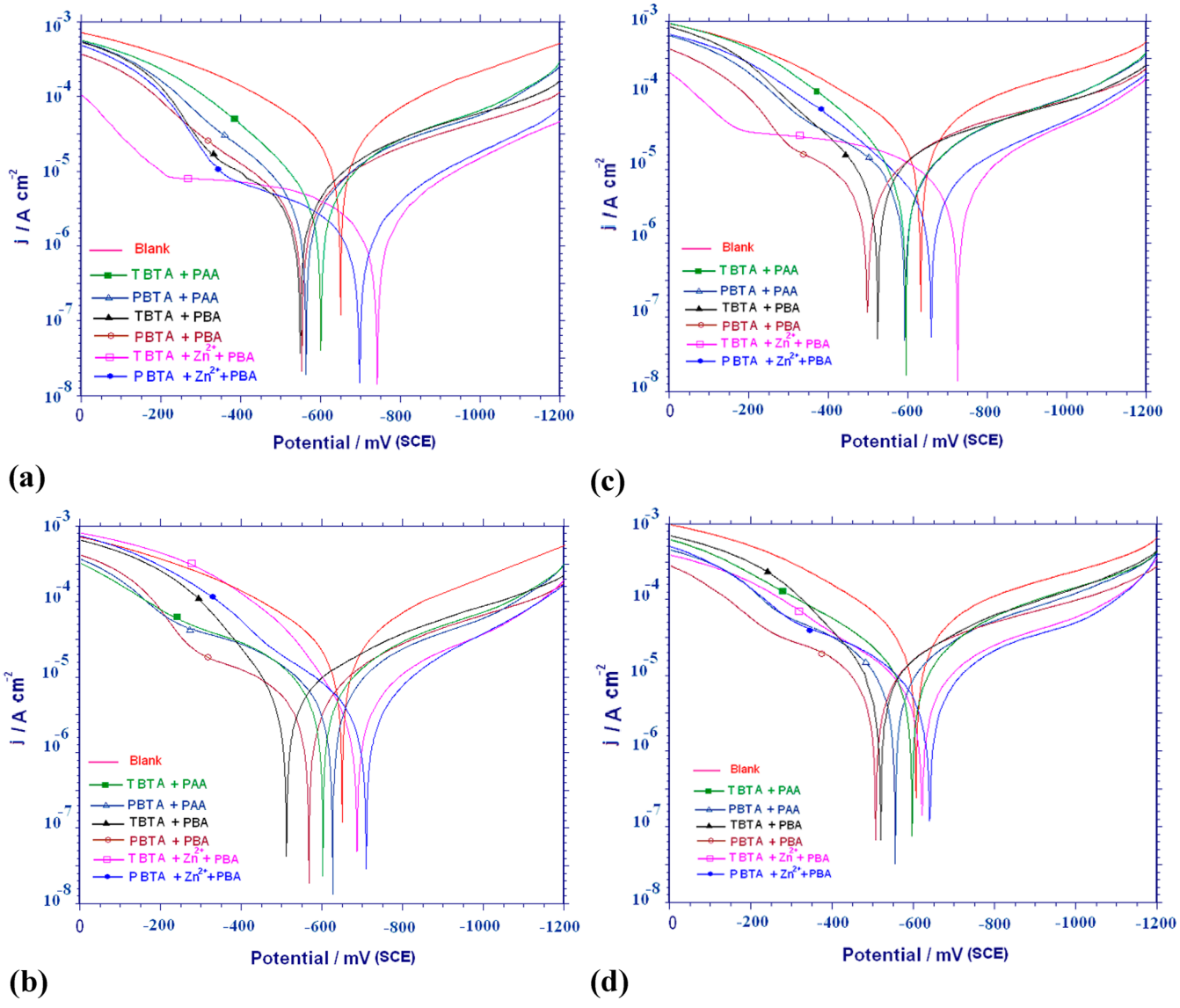

Figure 2. Potentiodynamic polarization curves of mild steel in groundwater in the absence and presence of optimum concentrations of TBTA + PAA, PBTA + PAA, TBTA + PBA, PBTA + PBA, TBTA + Zn^{2+} + PBA and PBTA + Zn^{2+} + PBA at (a) 30, (b) 40, (c) 50, and (d) 60 °C, respectively.

dx.doi.org/10.1021/ie4039357 | Ind. Eng. Chem. Res. 2014, 53, 4286−4294

Table 1. Potentiodynamic Polarization Parameters for Mild Steel Immersed in Groundwater in the Absence and Presence of Various Concentrations of TBTA, PBTA, Zn^{2+}, PAA and PBA in the Temperature Range 30−60 °C

		T = 30 °C			T = 40 °C			T = 50 °C			T = 60 °C		
inhibitor	concn [ppm]	E_{Corr} [mV]	j_{Corr} [μA cm^{-2}]	IE [%]	E_{Corr} [mV]	j_{Corr} [μA cm^{-2}]	IE [%]	E_{Corr} [mV]	j_{Corr} [μA cm^{-2}]	IE [%]	E_{Corr} [mV]	j_{Corr} [μA cm^{-2}]	IE [%]
blank	0	−640	12.59	–	−649	14.42	–	−635	16.79	–	−605	20.12	–
TBTA	10	−795	7.41	41.1	−715	8.78	39.1	−668	10.29	38.7	−750	12.35	38.6
	12	−744	6.12	51.4	−750	7.87	45.4	−758	8.65	48.5	−682	11.72	41.7
	14	−740	4.38	65.2	−719	5.76	60.0	−725	7.87	53.1	−752	9.87	50.9
	16	−775	3.55	71.8	−689	4.73	67.1	−672	6.25	62.8	−640	8.65	57.0
	18	−760	4.74	62.4	−784	6.26	56.5	−684	7.50	55.3	−701	9.53	52.6
	20	−725	5.60	55.5	−746	7.13	50.5	−715	8.78	47.7	−750	10.38	48.4
	22	−745	6.49	48.5	−749	8.25	42.7	−752	9.87	41.2	−766	12.41	38.3
PBTA	06	−715	7.08	43.8	−656	8.37	41.9	−668	10.29	38.7	−595	12.58	37.5
	08	−785	6.30	50.0	−693	6.33	56.1	−646	9.23	45.0	−580	10.36	48.5
	10	−715	5.82	53.8	−689	5.11	64.5	−633	7.23	56.9	−701	9.53	52.6
	12	−720	3.09	75.5	−672	4.24	70.7	−673	5.79	65.5	−637	8.23	59.1
	14	−748	4.16	66.9	−686	5.39	62.6	−646	6.83	59.3	−597	8.90	55.8
	16	−770	5.71	54.6	−646	6.83	52.7	−640	8.66	48.4	−525	10.36	48.5
	18	−774	6.96	44.7	−693	7.36	48.9	−615	10.19	47.9	−563	11.70	41.8
Zn^{2+}	30	−655	6.02	52.2	−735	7.50	47.9	−680	9.30	44.6	−692	11.27	43.9
	45	−690	5.62	55.4	−712	6.80	52.7	−758	8.65	48.4	−668	10.29	48.9
	60	−750	4.26	66.2	−654	6.59	54.9	−712	7.34	56.3	−723	10.01	50.2
	75	−705	3.98	68.4	−681	5.15	64.3	−666	6.73	59.9	−680	9.17	54.4
	90	−740	4.16	66.9	−692	6.26	56.6	−660	8.05	52.0	−752	9.87	50.9
	105	−740	4.78	62.0	−633	7.13	50.5	−640	8.66	48.4	−615	10.19	49.4
	120	−690	5.25	58.3	−615	7.58	47.4	−654	9.53	43.2	−689	11.66	42.0
PAA	06	−669	7.23	42.5	−625	8.29	42.5	−550	9.75	41.9	−521	11.55	42.6
	08	−744	6.38	49.3	−678	7.41	48.6	−556	8.91	46.9	−649	11.27	43.9
	10	−681	5.15	59.0	−654	6.49	54.9	−564	7.76	53.7	−519	10.21	48.9
	12	−627	4.71	62.6	−623	5.81	59.7	−625	7.34	56.3	−550	9.53	52.6
	14	−714	6.07	57.7	−515	6.83	52.6	−628	8.29	50.6	−580	10.36	48.5
	16	−713	6.42	49.0	−615	7.58	47.4	−597	8.90	46.9	−521	11.55	42.6
	18	−684	7.50	40.4	−549	8.41	41.6	−587	9.81	41.6	−538	12.24	39.2
PBA	04	−712	6.82	45.8	−553	8.35	42.1	−564	10.07	40.0	−595	12.58	37.4
	06	−744	6.38	49.3	−684	7.50	47.9	−597	8.91	47.8	−525	10.36	48.5
	08	−686	5.39	57.2	−693	6.33	56.1	−616	8.05	52.1	−554	9.72	51.7
	10	−618	3.77	70.1	−621	4.93	65.8	−599	6.45	61.6	−597	8.88	55.9
	12	−709	5.56	55.8	−646	6.83	52.6	−523	8.29	50.6	−587	9.80	51.2
	14	−672	6.68	46.9	−693	7.36	48.9	−641	8.45	49.6	−564	10.07	49.9
	16	−764	7.28	42.2	−621	7.78	46.0	−580	9.53	43.2	−682	11.72	41.7

as the reference electrode. Mild steel specimens with the weight percentage composition of C, 0.13%; P, 0.032%; Si, 0.014%; S, 0.025%; Mn, 0.48%; and balance Fe were used in this study. The mild steel for electrochemical measurements had dimensions of 1.0 cm length, 1.0 cm width, and 0.3 cm thickness and was prepared by attaching an insulated copper wire to one face of the sample, cold mounted in resin, and then left to dry in air for 24 h at room temperature. Before each experiment, the specimens were mechanically abraded with silicon carbide papers (from grades 120 to 1200), washed with distilled water, degreased with acetone, dried at room temperature, and then placed in the test solution.

Electrochemical Corrosion Measurements. All electrochemical measurements were performed at different temperatures (30, 40, 50, and 60 °C) using the Electrochemical Workstation Model No. CHI 760 (CH Instruments, USA). The platinum electrode and saturated calomel electrode (SCE) were used as auxiliary and reference electrodes, respectively, and the working electrodes constitute mild steel specimens of 1 cm^2 area. In order to minimize ohmic potential drop, the tip of the reference electrode is positioned in very close proximity to the working electrode surface by the use of a fine Luggin capillary, and the remaining uncompensated resistance was also reduced by the electrochemical workstation. For potentiodynamic polarization experiments, the potential was scanned from −1200 to 0.0 mV versus SCE at a scan rate of 0.1 mV s^{-1}. Electrochemical impedance spectroscopy (EIS) tests were performed after establishing the open-circuit potential (E_{Corr}) over a frequency range of 100 kHz−1 Hz, with an ac wave of ±5 mV peak-to-peak overlaid on a dc bias potential, and the impedance data were collected at a rate of 10 points per decade change in frequency.

Surface and Morphological Examinations. The corrosion products that were formed on the mild steel surface after its immersion for 7 days in groundwater in the absence and presence of inhibitors were identified by an X-ray diffractometer (XRD; Bruker D8 Advance, Germany). The surface morphology for the same mild steel coupons was also investigated using scanning electron microscopy (SEM; JEOL, Japan).

dx.doi.org/10.1021/ie4039357 | Ind. Eng. Chem. Res. 2014, 53, 4286−4294

RESULTS AND DISCUSSION

Potentiodynamic Polarization (PDP) Measurements. PDP curves of mild steel electrode after its immersion for 1 h in groundwater in the absence and presence of optimum concentrations of TBTA + PAA, PBTA + PAA, TBTA + PBA, PBTA + PBA, TBTA + Zn^{2+} + PBA, and PBTA + Zn^{2+} + PBA at 30 °C are shown in Figure 2a. The same measurements were performed for the mild steel at increased temperatures of 40, 50, and 60 °C, and the curves are shown in parts b, c, and d, respectively, of Figure 2. The values of the corrosion potential (E_{Corr}) and the corrosion current density (j_{Corr}) for the mild steel in all solutions were obtained from the extrapolation of

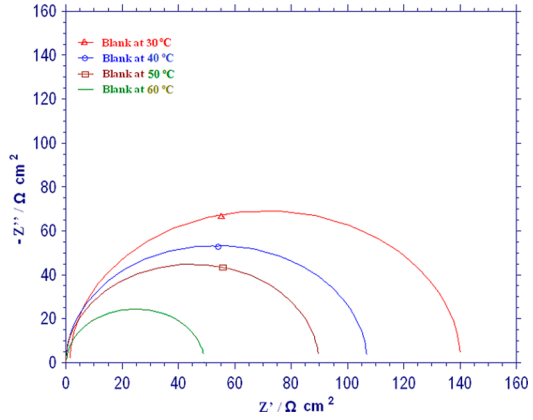

Figure 3. Nyquist plots obtained for mild steel after its immersion for 1 h in groundwater at various temperatures from 30 to 60 °C.

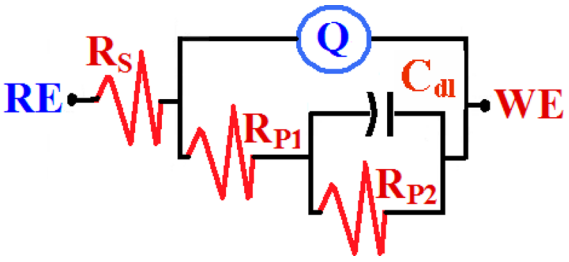

Figure 5. Equivalent circuit model used to fit the Nyquist plots shown in Figures 3 and 4. Definitions of symbols represented in the circuit are given in the text.

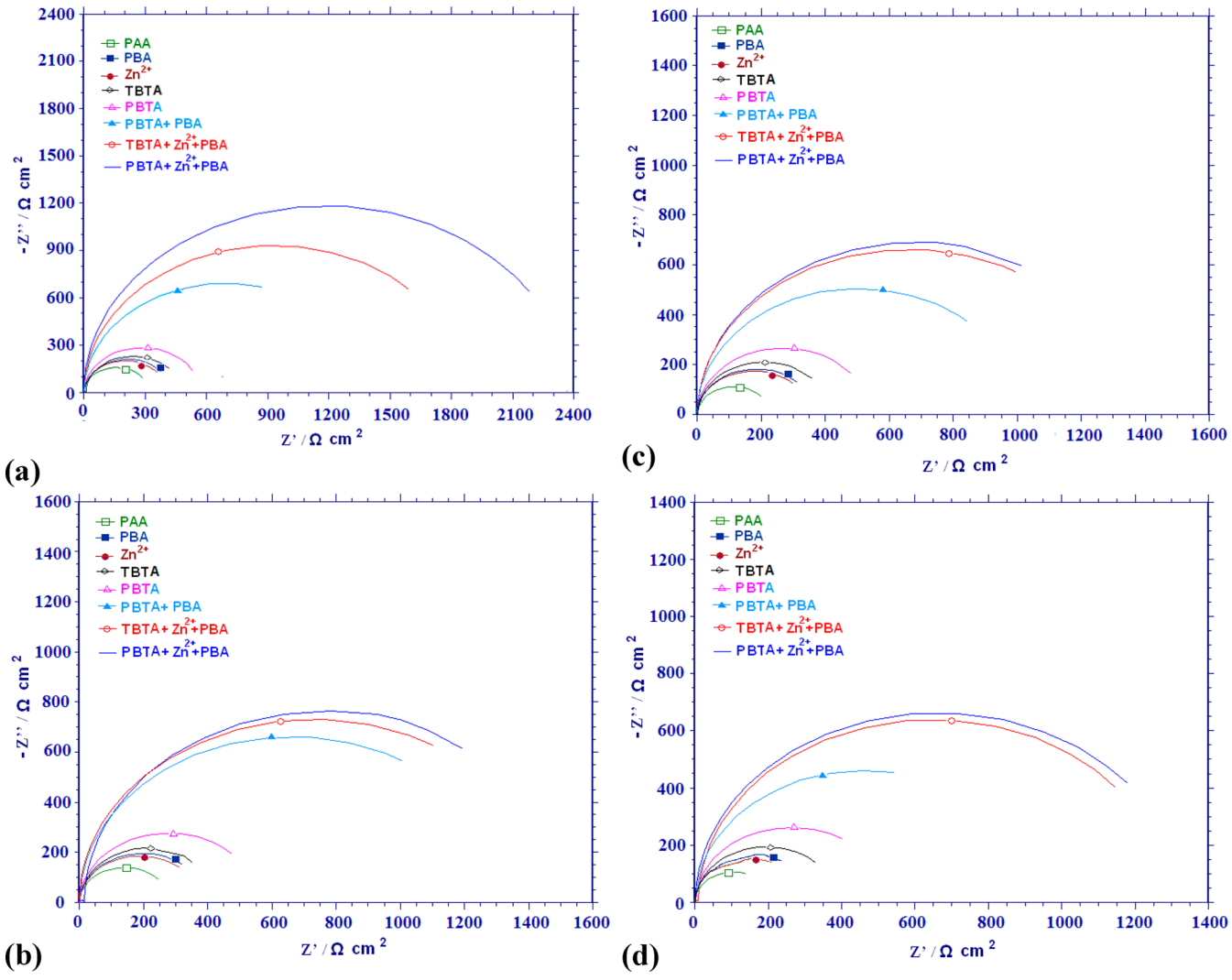

Figure 4. Nyquist plots obtained for mild steel after its immersion for 1 h in groundwater in the presence of optimum concentrations of various inhibitors at (a) 30, (b) 40, (c) 50, and (d) 60 °C, respectively.

dx.doi.org/10.1021/ie4039357 | Ind. Eng. Chem. Res. 2014, 53, 4286−4294

Table 2. Electrochemical Impedance Parameters for Mild Steel Immersed in Groundwater with Optimum Concentrations of Various Inhibitors in the Temperature Range 30−60 °C

	T = 30 °C			T = 40 °C		
inhibitor	R_{ct} [10^4 Ω cm^2]	C_{dl} [μF]	IE [%]	R_{ct} [10^4 Ω cm^2]	C_{dl} [μF]	IE [%]
blank	0.0130 ± 2.0	15.03 ± 0.05	−	0.0106 ± 2.0	18.24 ± 0.05	−
TBTA	0.4549 ± 2.0	7.05 ± 0.05	97.1	0.4362 ± 2.0	8.23 ± 0.05	97.6
PBTA	0.5728 ± 2.0	6.49 ± 0.05	97.7	0.5527 ± 2.0	7.61 ± 0.05	98.1
Zn^{2+}	0.3981 ± 2.0	7.42 ± 0.05	96.7	0.3703 ± 2.0	8.64 ± 0.05	97.1
PAA	0.3168 ± 2.0	7.83 ± 0.05	95.9	0.2784 ± 2.0	9.12 ± 0.05	96.2
PBA	0.4228 ± 2.0	7.24 ± 0.05	96.9	0.3905 ± 2.0	8.50 ± 0.05	97.3
TBTA + Zn^{2+}	1.2589 ± 2.0	6.11 ± 0.05	98.9	0.8925 ± 2.0	7.26 ± 0.05	98.8
PBTA + Zn^{2+}	1.2823 ± 2.0	5.81 ± 0.05	98.9	1.2680 ± 2.0	6.94 ± 0.05	99.2
PBTA + PAA	1.2790 ± 2.0	5.98 ± 0.05	98.9	0.9234 ± 2.0	7.13 ± 0.05	98.9
PBTA + PBA	1.3810 ± 2.0	5.24 ± 0.05	99.1	1.3250 ± 2.0	6.35 ± 0.05	99.2
PBTA+ Zn^{2+} + PAA	1.5316 ± 2.0	3.53 ± 0.05	99.2	1.3720 ± 2.0	4.61 ± 0.05	99.2
TBTA + Zn^{2+} + PBA	1.8620 ± 2.0	2.31 ± 0.05	99.3	1.4600 ± 2.0	3.54 ± 0.05	99.3
PBTA + Zn^{2+} + PBA	2.3605 ± 2.0	1.72 ± 0.05	99.5	1.5310 ± 2.0	2.91 ± 0.05	99.3
	T = 50 °C			T = 60 °C		
inhibitor	R_{ct} [10^4 Ω cm^2]	C_{dl} [μF]	IE [%]	R_{ct} [10^4 Ω cm^2]	C_{dl} [μF]	IE [%]
blank	0.0084 ± 2.0	22.62 ± 0.05	−	0.0048 ± 2.0	27.41 ± 0.05	−
TBTA	0.4196 ± 2.0	9.12 ± 0.05	98.0	0.3874 ± 2.0	12.20 ± 0.05	98.8
PBTA	0.5332 ± 2.0	8.45 ± 0.05	98.4	0.5244 ± 2.0	11.72 ± 0.05	98.1
Zn^{2+}	0.3488 ± 2.0	9.64 ± 0.05	97.6	0.3294 ± 2.0	12.90 ± 0.05	98.5
PAA	0.2233 ± 2.0	10.21 ± 0.05	96.2	0.2099 ± 2.0	13.34 ± 0.05	97.7
PBA	0.3649 ± 2.0	9.43 ± 0.05	97.7	0.3342 ± 2.0	12.51 ± 0.05	98.6
TBTA + Zn^{2+}	0.6119 ± 2.0	8.19 ± 0.05	98.6	0.5244 ± 2.0	11.31 ± 0.05	98.1
PBTA + Zn^{2+}	0.9154 ± 2.0	7.81 ± 0.05	99.1	0.8899 ± 2.0	10.76 ± 0.05	99.5
PBTA + PAA	0.6733 ± 2.0	8.08 ± 0.05	98.6	0.5725 ± 2.0	11.10 ± 0.05	99.2
PBTA + PBA	1.0091 ± 2.0	7.26 ± 0.05	99.2	0.9234 ± 2.0	10.23 ± 0.05	99.5
PBTA + Zn^{2+} + PAA	1.2810 ± 2.0	5.42 ± 0.05	99.3	1.0350 ± 2.0	8.43 ± 0.05	99.5
TBTA + Zn^{2+} + PBA	1.3252 ± 2.0	4.31 ± 0.05	99.4	1.2579 ± 2.0	7.45 ± 0.05	99.6
PBTA + Zn^{2+} + PBA	1.3971 ± 2.0	3.62 ± 0.05	99.4	1.3251 ± 2.0	5.14 ± 0.05	99.6

Table 3. Electrochemical Impedance Parameters Obtained from Equivalent Circuit Shown in Figure 5 for Mild Steel Immersed in Groundwater with Optimum Concentration of PBTA + Zn^{2+} + PBA in the Temperature Range 30−60 °C

		Q					
T [°C]	R_S [Ω cm^2]	Y_Q [μF cm^{-2}]	n	R_{P1} [10^4 Ω cm^2]	C_{dl} [μF]	R_{P2} [10^4 Ω cm^2]	C [μF cm^{-2}]
30	14.65	0.0099	0.8	2.3605	1.72 ± 0.05	1.47	0.39
40	13.87	0.0284	0.8	1.5310	2.91 ± 0.05	1.25	0.45
50	12.79	0.0865	0.78	1.3971	3.62 ± 0.05	0.98	0.55
60	10.97	0.1570	0.82	1.3251	5.14 ± 0.05	0.87	0.71

anodic and cathodic Tafel lines located next to the linearized current regions. These values in addition to the value of the percentages of the inhibition efficiency (IE) are listed in Table 1. It is worth mentioning also that the PDP curves were collected for the steel in groundwater that contained concentrations of PBTA, TBTA, PBA, and PAA varying from 4 to 22 ppm, while for Zn^{2+} the concentrations ranged between 30 and 120 ppm; this is also listed in Table 1. The recorded values of the IE were calculated according to the following equation:[23]

$$\mathrm{IE}\ (\%) = \frac{j_{\mathrm{Corr}} - j^{\circ}_{\mathrm{Corr}}}{j_{\mathrm{Corr}}} \cdot 100 \quad (1)$$

where j_{Corr} and $j^{\circ}_{\mathrm{Corr}}$ are the corrosion current densities in the absence and presence of inhibitor, respectively.

It is clearly seen from Figure 2a and Table 1 that the mild steel in groundwater in the absence of any inhibitor showed the highest cathodic and anodic currents and j_{Corr} value. It is generally believed that the cathodic reaction for iron and steel alloys is the oxygen reduction as follows.

$$O_2 + 2H_2O + 4e^- = 4OH^- \quad (2)$$

On the other hand, the anodic reaction has been reported[23] to be the dissolution of iron to ferrous cations, which in turn transfer to ferric cations.

$$Fe = Fe^{2+} + 2e^- \quad (3)$$

$$Fe^{2+} = Fe^{3+} + e^- \quad (4)$$

These reactions are activated with the increase of the applied potential in the anodic direction and in the presence of oxygen, which leads to the corrosion of the steel and the formation of a top layer of oxides on its surface.[23]

$$2Fe + O_2 + 2H_2O = 2Fe(OH)_2 \quad (5)$$

dx.doi.org/10.1021/ie4039357 | Ind. Eng. Chem. Res. 2014, 53, 4286−4294

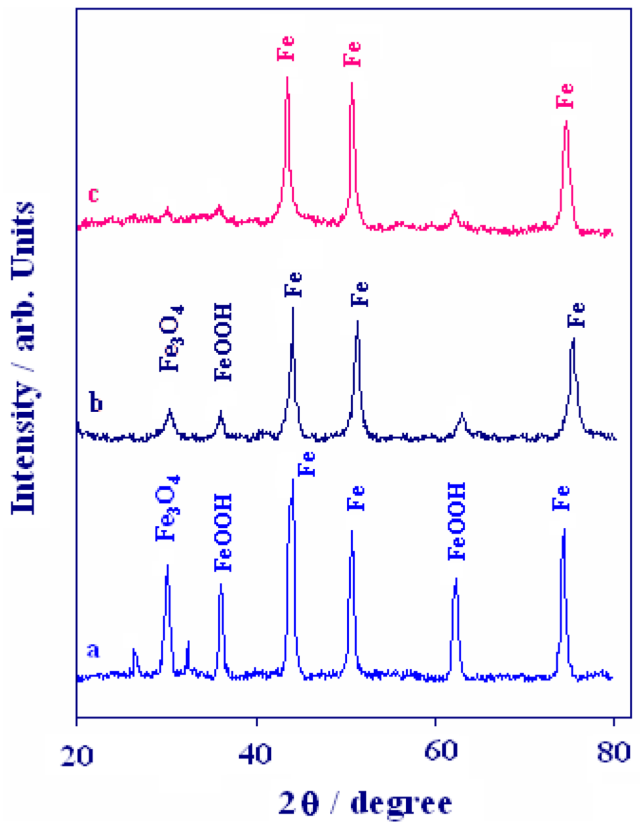

Figure 6. XRD pattern obtained on the surface of mild steel in the groundwater containing (a) no inhibitor, (b) PBTA + PBA, and (c) PBTA+ Zn^{2+} + PBA at 30 °C.

$$3Fe(OH)_2 + \frac{1}{2}O_2 = Fe_3O_4 + 3H_2O \tag{6}$$

Addition of PBTA up to the optimum level shows a consistent decrease in the anodic and cathodic currents and the value j_{Corr} (see Table 1) compared to those recorded for the steel in groundwater alone. This proves that PBTA acts as a mixed type inhibitor with a predominant anodic effect due to the adsorption of its molecules on the surface. Furthermore, the addition of zinc along with PBTA did not modify the mechanism of the process; however, it slightly altered the shape of the anodic curve as a result of the predominant cathodic inhibition of zinc. The presence of active sites such as aromatic rings and heteroatoms in the benzotriazole derivatives is responsible for the adsorption.[11] This effect was found to increase with increasing the inhibitor concentration and confirmed by increasing the value of IE with the inhibitor concentration up to the optimum level due to the increase of the amount of adsorbed inhibitor. The optimum concentrations were evaluated based on the inhibition efficiency, and the combination of benzotriazole derivatives with Zn^{2+} and phosphono derivatives were also studied.

It is also seen from Figure 2a and Table 1 that the value of E_{Corr} shifted to the more negative direction for all the individual inhibitors except PAA and PBA, for which the shift in the E_{Corr} value is positive. The individual inhibitors, except PAA, PBA, and PBTA, act as mixed type inhibitors with moderate control of the cathodic reaction. While the value of E_{Corr} in the presence of benzotriazole derivatives and Zn^{2+} showed a shift in the negative direction, the phosphono derivatives with Zn^{2+} showed a shift in the positive direction when compared with

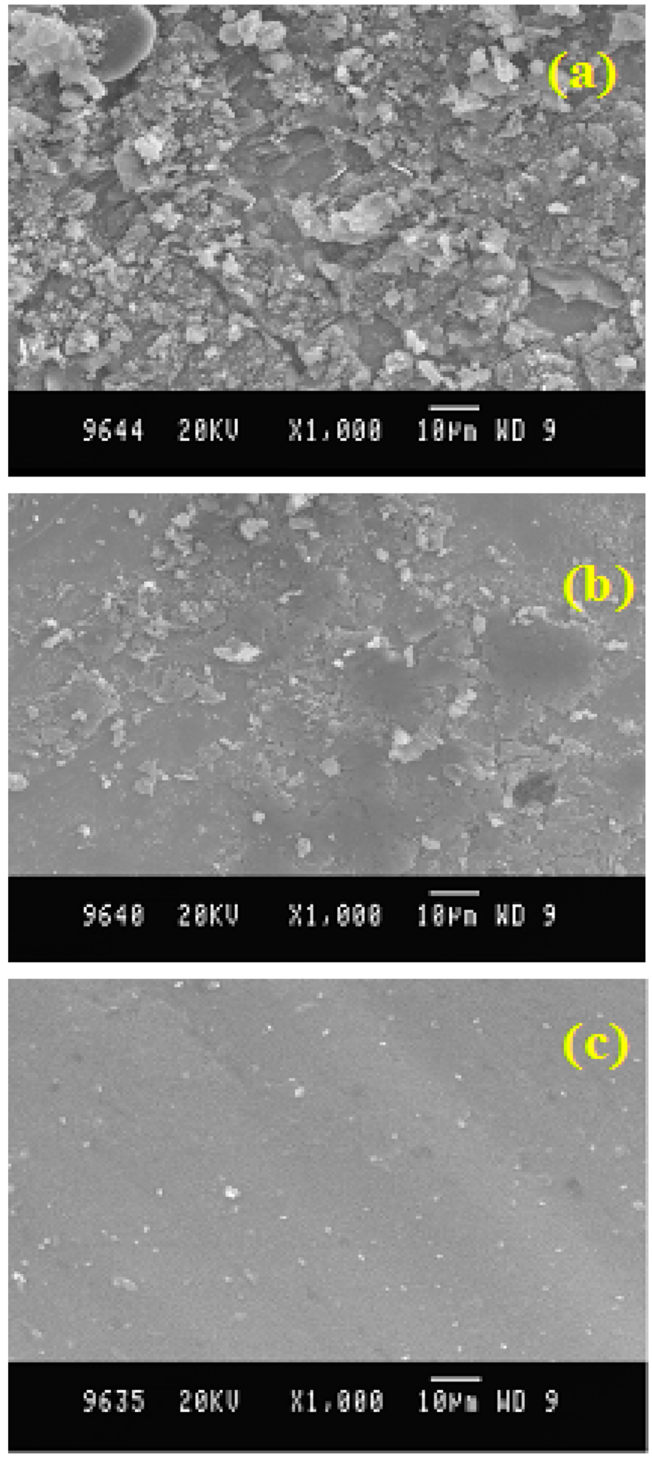

Figure 7. SEM micrographs of (a) blank, (b) presence of PBTA + PBA, and (c) presence of PBTA + Zn^{2+} + PBA at 30 °C.

the groundwater alone. The negative E_{Corr} shift demonstrates the cathodic inhibiting effect of the combination of both PBTA and TBTA with Zn^{2+}.

Table S2 (Supporting Information) shows the variations of E_{Corr}, j_{Corr}, and IE for the mild steel in groundwater in the absence and presence of the different inhibitors and zinc at 40, 50, and 60 °C. It is obvious from Figure 2b–d and Table S2 in the Supporting Information that the j_{Corr} increased by 1 order of magnitude with increasing temperature, in both uninhibited and inhibited systems. On the other hand, the j_{Corr} values

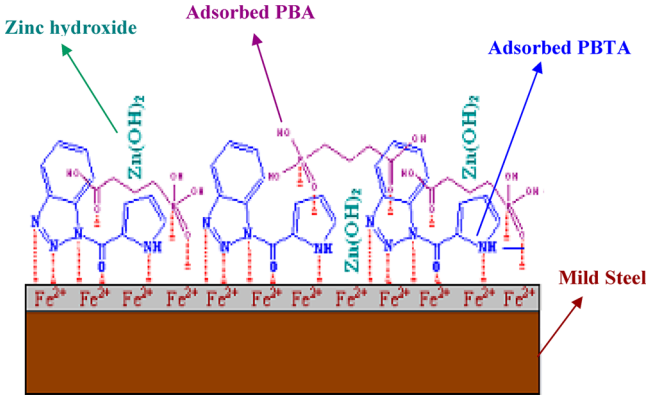

Figure 8. Proposed model of the adsorption process of PBTA, Zn^{2+}, and PBA on the mild steel surface.

decreased significantly in the presence of benzotriazole derivatives when the temperature was not changed. Further, the binary combination of each benzotriazole derivative with Zn^{2+} was found to be acting as an inhibitor more effectively than the individual ones. In the presence of Zn^{2+} and PBA at 30 °C, the values of IE for TBTA and PBTA were increased to 89.3 and 91.5%, respectively. In the presence of a ternary inhibitor system, the E_{Corr} value tends toward positive potential values and the inhibition efficiency decreases considerably with increasing temperature. Correlating the values obtained for individual inhibitors with those of the combinations, it is evident that the addition of Zn^{2+} along with either of the phosphonic acid derivatives PAA and PBA to the benzotriazole derivatives controls the cathodic and anodic reactions; therefore, it can be concluded that benzotriazole derivatives act as mixed type inhibitors even with the increase of temperature. The j_{Corr} increased by 1 order of magnitude with increasing temperature, in both uninhibited and inhibited systems. According to the Arrhenius equation, the activation energy of metal dissolution in the absence and presence of inhibitor can be calculated as follows.

$$E_a = 2.303R\frac{T_1T_2}{T_2 - T_1}\log(\rho_2/\rho_1) \quad (7)$$

where ρ_1 and ρ_2 are the corrosion rates at temperatures T_1 and T_2, respectively. The calculated activation energies are recorded in Table S3 (Supporting Information), which states that the values of E_a are higher in the presence of inhibitor when compared with values for the groundwater alone. In the literature,[24] the lower activation energy value of the corrosion process in the presence of an inhibitor is attributed to its chemisorption, while it is found to be opposite in the case with physical adsorption. It is also reported[24] that the energy barrier of the corrosion process increases in the presence of benzotriazole derivatives. E_a increased in the presence of the inhibitor in aqueous media, suggesting that the adsorbed organic molecules create a physical barrier to charge and mass transfer, leading to a reduction in the corrosion rate.[25]

All PDP results show that the benzotriazole compounds are initially adsorbed on the metal surface and then the addition of PAA and/or PBA leads to the formation of iron(II) phosphonate complex as a protective layer, which enhances the corrosion inhibition efficiency.[11] This confirms that the combination of benzotriazole compounds (TBTA or PBTA) along with Zn^{2+} and either PAA or PBA provides increased corrosion inhibition for the steel surface.

Electrochemical Impedance Spectroscopy (EIS) Measurements. EIS Nyquist plots recorded at open-circuit potential for the mild steel after its immersion for 1 h in groundwater alone at different temperatures are shown in Figure 3. Similar Nyquist plots were also recorded for the mild steel in the absence and the presence of various optimum inhibitor concentrations at different temperatures, from 30 to 60 °C, and are shown in Figure 4. The EIS data were best fitted to the equivalent circuit model shown in Figure 5. The symbols of the equivalent circuit can be defined as follows: R_S represents the solution resistance, R_{P1} represents the polarization resistance and is also defined as the charge transfer resistance due to the oxidation of the steel surface, Q is the constant phase elements (CPE), C_{dl} represents the capacitance of the inhibitor film on the metal surface due to adsorption, and R_{P2} is another polarization resistance that corresponds to the formed film on the steel surface and solution interface. The values of the symbols of the equivalent circuit that were evaluated using a fitting procedure,[26] in addition to the values of the values of IE, which were calculated as reported in our previous work,[15] are listed in Table 2. It is clearly seen from Figure 3 that the Nyquist plots do not show perfect semicircles: the diameter decreased with increasing the temperature of the groundwater and this difference has been attributed to the frequency dispersion.[27] This agrees with the polarization data that increasing the temperature of the groundwater decreases the corrosion resistance of the steel and thus increases its dissolution. This was also confirmed by the decrease of R_{ct} and the increase of C_{dl} values with increasing temperature as can be seen from Table 2.

The Nyquist plots shown in Figure 4 indicate that the values of charge transfer resistance for the individual inhibitors increase in the order PAA < Zn^{2+} < PBA < TBTA < PBTA. When this is compared to the blank, the capacitance values show an appreciable decrease in the reverse order. In the combination of PBTA and Zn^{2+} a further increase in the charge transfer resistance was also noted and this value reached a maximum for PBTA + Zn^{2+} + PBA, demonstrating that this combination provides the maximum corrosion protection; the same trend was noted for all temperatures (30−60 °C). Simultaneous increase of the charge transfer resistance and decrease of the double layer capacitance with increasing inhibitor concentration indicates that these compounds inhibit the corrosion rate of mild steel by an adsorption mechanism.[28] The decrease in C_{dl} is due to the adsorption of this compound on the metal surface leading to the formation of a surface film in the aqueous solution.[29] The Bode plots for mild steel immersed in groundwater with optimum concentration of PBTA + Zn^{2+} + PBA in the temperature range 30−60 °C as shown in Figure S1 (Supporting Information) exhibit one time constant, thus showing that the inhibitor system behaves as a monolayer formation and the dissolution process is controlled by a charge transfer reaction.

The values of all EIS parameters appearing on the equivalent circuit (Figure 5) were obtained for the mild steel in the groundwater containing the optimum concentration of PBTA + Zn^{2+} + PBA mixture, which showed the best performance in inhibiting corrosion at the different temperatures. The values are listed in Table 3. Furthermore, the values of the capacitance (C) over the whole frequency range were calculated according to eq 8 and appear in Table 3.

$$C = (QR^{1-n})^{1/n} \quad (8)$$

dx.doi.org/10.1021/ie4039357 | Ind. Eng. Chem. Res. 2014, 53, 4286−4294

where Q is the CPE constant [F cm^{-2}], n is the value accompanying the CPE (see Table 3), and R is the charge transfer resistance. It is clearly seen from Table 3 that the values of R_S, R_{P1}, and R_{P2} decrease with increasing temperature from 30 to 60 °C due to the fact that the increase of temperature increases the activation of the mild steel surface and thus increases its corrosion. On the other hand, and with these decreases, the presence of the optimum concentration of PBTA + Zn^{2+} + PBA decreases the dissolution effect of increasing temperature as indicated by the increased values of IE as shown in Table 2. The CPE represent double layer capacitors with their n values of ca. 0.8 and also the C_{dl} values increase with increasing temperature, which was expected as a result of decreasing the coverage of the charged surfaces. The EIS data thus show the same trend as those observed from dc polarization measurements.

X-ray Diffraction Patterns. The XRD patterns of the corrosion products give qualitative information about the possible phases present. The patterns obtained clearly reveal the presence of metal and metal oxide phases. The XRD results are presented in Figure 6. The peaks due to iron appear at 2θ = 43.8, 60.1, and 74.5°. Peaks at 2θ = 30.4, 35.9, and 62.5° can be assigned to oxides of iron. Thus, the surface of the metal immersed in groundwater contains iron oxides, which are most probably Fe_3O_4 and FeOOH. The XRD pattern for the metal immersed in the groundwater containing optimum concentration of PBTA + Zn^{2+} + PBA is given in Figure 6c. The intensity of the peaks due to oxides of iron, such as Fe_3O_4 and FeOOH, are found to be very low and the peaks due to iron alone observed at 2θ = 43.7, 50.9, and 74.3° are very high.

SEM Surface Investigations. Figure 7 shows SEM micrographs for mild steel that was exposed to (Figure 7a) groundwater alone, (Figure 7b) groundwater containing optimum concentration of PBTA + PBA, and (Figure 7c) groundwater containing optimum concentration of PBTA + Zn^{2+} + PBA at 30 °C. For the steel in groundwater alone (Figure 7a) the SEM micrograph shows that the surface is highly damaged and flakes are seen. This is due to the formation of corrosion products, which were most probably iron hydroxides and oxides as previously represented by eqs 5 and 6. The SEM image for the mild steel in groundwater containing optimum concentration of PBTA + PBA (Figure 7b) shows reduced deterioration, whereas the SEM image for the mild steel in groundwater containing optimum concentration of PBTA + Zn^{2+} + PBA (Figure 7c) exhibits no such obvious deterioration. This clearly indicates that the mixture of inhibitors PBTA + Zn^{2+} + PBA effectively protects the mild steel surface from aggressive solution.

Mechanism of Inhibition. According to the obtained results, the inhibition of mild steel in groundwater medium by the tested inhibitors can be explained on the basis of the adsorption process.[11,30] It is reported[31] that the strength of adsorption is affected by number of adsorption sites, charge density, molecular size, and mode of interactions with the metal surface and the stability of the film to be formed. Here, the adsorption of the inhibitor compounds on the mild steel surface could occur directly on the basis of donor−acceptor behavior between the lone pairs of the heteroatom and the extensively delocalized π-electrons of the inhibitor molecule and the vacant d-orbital of iron surface atoms.[32] These compounds are able to be adsorbed on anodic sites through N and O atoms, heterocyclic rings, and aromatic rings, which are electron donating groups. Thus, the adsorption of these compounds on the steel surface decreases its anodic reactions by blocking the active sites and therefore decreases the anodic dissolution of mild steel.

The possible adsorption mechanism of benzotriazole derivatives, Zn^{2+}, and phosphono derivatives is proposed in the model illustrated in Figure 8. It is indicated from obtained data that the inhibition efficiency increases with the addition of Zn^{2+}. This may be due to the coadsorption of benzotriazole derivatives and phosphono derivatives, which is either competitive or cooperative.[33] In competitive adsorption, these benzotriazole and phosphono derivatives may be adsorbed at different sites on the metal surface.[34] In this case, the adsorption of anionic species enhances the adsorption of cationic and neutral species and vice versa. In cooperative adsorption, the electron-rich species is chemisorbed on the metal surface and the neutral or low electron negative species is adsorbed on the chemisorbed layer. Hence, both competitive and cooperative adsorption mechanisms may occur simultaneously.[35] However, the results obtained in the present work indicate that the competitive adsorption between the benzotriazole derivatives with Zn^{2+} and phosphono derivatives dominates over the cooperative adsorption.

■ CONCLUSION

The results revealed that the studied compounds are good inhibitors for mild steel corrosion in aqueous media. The synthesized benzotriazole derivatives (PBTA and TBTA) were found to suppress the anodic and cathodic reactions and hence behave as mixed type inhibitors. On the basis of temperature dependence of the inhibition efficiency, all the studied compounds were found to be physically adsorbed on the mild steel surface. The effect of temperature on the inhibition efficiency of the inhibitor combinations is less pronounced even on increasing the temperature. Hence, a good inhibition is ensured at elevated temperatures. SEM micrographs ensured that the adsorption of optimum concentration of benzotriazole derivative and iron(II) phosphonate complex on the surface of mild steel in the PBTA + Zn^{2+} + PBA system protects the mild steel well from aggressive solution rather more than other combinations. PBTA + Zn^{2+} + PBA formulation showed the highest IE at all the temperatures, i.e., 91.5, 88.1, 82.3 and 74.1% for 30, 40, 50, and 60 °C, respectively.

■ ASSOCIATED CONTENT

Supporting Information

Chemical composition of groundwater (Table S1), potentiodynamic polarization parameters for mild steel immersed in groundwater media in the presence and absence of optimum concentrations of TBTA + Zn^{2+}, PBTA + Zn^{2+}, PBTA + PAA, PBTA + PBA, TBTA + Zn^{2+} + PAA, PBTA + Zn^{2+} + PAA, TBTA + Zn^{2+} + PBA, and PBTA + Zn^{2+} + PBA in the temperature range 30−60 °C (Table S2), energy of activation for the corrosion of mild steel in aqueous media in the absence and presence of optimum concentrations of various inhibitors at different temperatures (Table S3), and Bode plots obtained for mild steel immersed in groundwater with optimum concentration of PBTA + Zn^{2+} + PBA in the temperature range 30−60 °C (Figure S1). This material is available free of charge via the Internet at http://pubs.acs.org.

dx.doi.org/10.1021/ie4039357 | Ind. Eng. Chem. Res. 2014, 53, 4286−4294

AUTHOR INFORMATION

Corresponding Author

*Tel.: +91 427 2345766. Fax: +91 427 2345124. E-mail: dhanaraj_gopi@yahoo.com.

Notes

The authors declare no competing financial interest.

ACKNOWLEDGMENTS

D.G. gratefully acknowledges the University Grants Commission (UGC-F No.40-64/2011 (SR)), New Delhi, India, for the financial support in the form of major research project. Also, D.G. and L.K. acknowledge the UGC (Ref. No. F. 30-1/2013(SA-II)/RA-2012-14-NEW-SC-TAM-3240 and Ref. No. F. 30-1/2013(SA-II)/RA-2012-14-NEW-SC-TAM-3228) for the Research Award. D.R. acknowledges the major financial support from the Department of Science and Technology, New Delhi, India (DST-Ref. No. SR/WOS-A/PS-26/2012 (G)).

REFERENCES

(1) Gopi, D.; Govindaraju, K. M.; Prakash, V. C. A.; Angeline Sakila, D. M.; Kavitha, L. A study on new benzotriazole derivatives as inhibitors on copper corrosion in ground water. *Corros. Sci.* **2009**, *51*, 2259−2265.

(2) Döner, A.; Solmaz, R.; Özcan, M.; Kardaş, G. Experimental and theoretical studies of thiazoles as corrosion inhibitors for mild steel in sulphuric acid solution. *Corros. Sci.* **2011**, *53*, 2902−2913.

(3) Kustu, C.; Emregul, C. K.; Atakol, O. Schiff bases of increasing complexity as mild steel corrosion inhibitors in 2M HCl. *Corros. Sci.* **2007**, *49*, 2800−2814.

(4) Umoren, S. A.; Gasem, Z. M.; Obot, I. B. Natural products for material protection: Inhibition of mild steel corrosion by date palm seed extracts in acidic media. *Ind. Eng. Chem. Res.* **2013**, *52*, 14855−14865.

(5) Krishnaveni, K.; Ravichandran, J.; Selvaraj, A. Inhibition of mild steel corrosion by Morinda tinctoria leaves extract in sulphuric acid medium. *Ionics* **2013**, *20*, 115−126.

(6) Babić-Samardž, K.; Hackerman, N. Triazole, benzotriazole and substituted benzotriazoles as corrosion inhibitors of iron in aerated acidic media. *J. Solid State Electrochem.* **2005**, *9*, 483−497.

(7) Aramaki, K.; Kiuchi, T.; Sumiyoshi, T.; Nishihara, H. Studies on the inhibition of copper corrosion in sulfate solutions by 5-substituted benzotriazoles. *Corros. Sci.* **1991**, *32*, 593−607.

(8) Al-Muhanna, K.; Habib, K. Corrosion behavior of different alloys exposed to continuous flowing seawater by electrochemical impedance spectroscopy (EIS). *Desalination* **2010**, *250*, 404−407.

(9) Tao, Z.; He, W.; Wang, S.; Zhou, G. Electrochemical study of cyproconazole as a novel corrosion inhibitor for copper in acidic solution. *Ind. Eng. Chem. Res.* **2013**, *52*, 17891−17899.

(10) Gopi, D.; Govindaraju, K. M.; Prakash, V. C. A.; Manivannan, V.; Kavitha, L. Inhibition of mild steel corrosion in groundwater by pyrrole and thienylcarbonyl benzotriazoles. *J. Appl. Electrochem.* **2009**, *39*, 269−276.

(11) Govindaraju, K. M.; Gopi, D.; Kavitha, L. Inhibiting effects of 4-amino-antipyrine based Schiff base derivatives on the corrosion of mild steel in hydrochloric acid. *J. Appl. Electrochem.* **2009**, *39*, 2345−2352.

(12) Gopi, D.; Manimozhi, S.; Govindaraju, K. M.; Manisankar, P.; Rajeswari, S. Surface and electrochemical characterization of pitting corrosion behavior of 304 stainless steel in ground water media. *J. Appl. Electrochem.* **2007**, *37*, 439−449.

(13) Gopi, D.; Govindaraju, K. M.; Manimozhi, S.; Ramesh, S.; Rajeswari, S. Inhibitors with biocidal functionalities to mitigate corrosion on mild steel in natural aqueous environment. *J. Appl. Electrochem.* **2007**, *37*, 681−689.

(14) Wippermann, K.; Schultze, J.; Kessel, R.; Penninger, J. The inhibition of zinc corrosion by bisaminotriazole and other triazole derivatives. *Corros. Sci.* **1991**, *32*, 205−223.

(15) Sherif, E. M. Corrosion inhibition in 2.0 M sulfuric acid solutions of high strength maraging steel by aminophenyl tetrazole as a corrosion inhibitor. *Appl. Surf. Sci.* **2014**, *292*, 190−196.

(16) Gunasekaran, G.; Palaniswamy, N.; Apparao, B. V.; Muralidharan, V. S. Synergistic inhibition in low chloride media. *Electrochim. Acta* **1997**, *42*, 1427−1434.

(17) Gopi, D.; Rajeswari, S. Surface characterization and electrochemical corrosion behavior of 304 stainless steel in aqueous media. *J. Solid State Electrochem.* **2002**, *6*, 194−202.

(18) Telegdi, J.; Kalman, E. H.; Karman, F. Corrosion and scale inhibitors with systematically changed structure. *Corros. Sci.* **1992**, *33*, 1099−1103.

(19) Sekine, I.; Hirakawa, Y. Corrosion of copper metal in presence of binary mixtures. *Corrosion* **1986**, *42*, 271.

(20) Katritzky, A. R.; Wang, Z.; Wang, M.; Wilkerson, C. R.; Hall, C. D.; Akhmedov, N. G. Preparation of β-keto esters and β-diketones by C-acylation/deacetylation of acetoacetic esters and acetonyl ketones with 1-acylbenzotriazoles. *J. Org. Chem.* **2004**, *69*, 6617−6622.

(21) Wang, X.; Zhang, Y. Samarium diiodide promoted formation of 1,2-diketones and 1-acylamido-2-substituted benzimidazoles from *N*-acylbenzotriazoles. *Tetrahedron* **2003**, *59*, 4201−4207.

(22) Langelier, W. F. The analytical control of anti-corrosion water treatment. *J.—Am. Water Works Assoc.* **1936**, *28*, 1500−1521.

(23) Sherif, E. M. Comparative Study on the inhibition of iron corrosion in aerated stagnant 3.5 wt % sodium chloride solutions by 5-phenyl-1H-tetrazole and 3-amino-1,2,4-triazole. *Ind. Eng. Chem. Res.* **2013**, *52*, 14507−14513.

(24) Larabi, L.; Harek, Y.; Benali, O.; Ghalem, S. Erratum to "Hydrazide derivatives as corrosion inhibitors for mild steel in 1 M HCl" [Prog. Org. Coat. 54 (2005) 256−262]. *Prog. Org. Coat.* **2006**, *57*, 170.

(25) Oguzie, E. E. Studies on the inhibitive effect of *Occimum viridis* extract on the acid corrosion of mild steel. *Mater. Chem. Phys.* **2006**, *99*, 441−446.

(26) Egand, G. *Basics of A.C. Impedance Measurements*; Application Note AC-1; Princeton Applied Research:: Oak Ridge, TN, 1982.

(27) Mansfeld, F.; Kending, M. W.; Tsai, S. Recording and analysis of AC impedance data for corrosion studies: II. Experimental approach and results. *Corros. Sci.* **1982**, *38*, 570−579.

(28) Quraishi, M. A. Influence of iodide ions on inhibitive performance of tetraphenyl-dithia-octaaza-cyclotetradeca-hexaene (PTAT) during pickling of mild steel in hot sulfuric acid. *Mater. Chem. Phys.* **2001**, *70*, 95−99.

(29) Bentiss, F.; Lagrenee, M.; Traisnel, M.; Hornez, J. The corrosion inhibition of mild steel in acidic media by a new triazole derivative. *Corros. Sci.* **1999**, *41*, 789−803.

(30) Schweinsgberg, D.; George, G.; Nanayakkawa, A.; Steinert, D. The protective action of epoxy resins and curing agents—inhibitive effects on the aqueous acid corrosion of iron and steel. *Corros. Sci.* **1988**, *28*, 33−42.

(31) Fouda, A.; Moussa, M.; Taha, F.; Neanaa, I. The role of some thiosemicarbazide derivatives in the corrosion inhibition of aluminium in hydrochloric acid. *Corros. Sci.* **1986**, *26*, 719−726.

(32) Muralidharan, S.; Quraishi, M. A.; Iyer, S. V. K. The effect of molecular structure on hydrogen permeation and the corrosion inhibition of mild steel in acidic solutions. *Corros. Sci.* **1995**, *37*, 1739−1750.

(33) Schmitt, G.; Bedlur, K. Investigations on structural and electronic effects in acid inhibitors by AC impedance. *Werkst. Korros.* **1985**, *36*, 273−278.

(34) Karakus, M.; Sahin, M.; Bilgic, S. An investigation on the inhibition effects of some new dithiophosphonic acid monoesters on the corrosion of the steel in 1 M HCl medium. *Mater. Chem. Phys.* **2005**, *92*, 565−571.

(35) Oguzie, E. E.; Li, Y.; Wang, F. H. Corrosion inhibition and adsorption behavior of methionine on mild steel in sulfuric acid and synergistic effect of iodide ion. *J. Colloid Interface Sci.* **2007**, *310*, 90−98.